

## Upgrades to improve the usability, reliability, and spectral range of the MST Thomson scattering diagnostic

S. Z. Kubala, M. T. Borchardt, D. J. Den Hartog, D. J. Holly, C. M. Jacobson, L. A. Morton, and W. C. Young

Citation: *Rev. Sci. Instrum.* **87**, 11E547 (2016); doi: 10.1063/1.4962251

View online: <http://dx.doi.org/10.1063/1.4962251>

View Table of Contents: <http://aip.scitation.org/toc/rsi/87/11>

Published by the [American Institute of Physics](#)

---

---



# Upgrades to improve the usability, reliability, and spectral range of the MST Thomson scattering diagnostic

S. Z. Kubala,<sup>a)</sup> M. T. Borchardt, D. J. Den Hartog, D. J. Holly, C. M. Jacobson, L. A. Morton, and W. C. Young

*Department of Physics, University of Wisconsin-Madison, Madison, Wisconsin 53706, USA*

(Presented 8 June 2016; received 6 June 2016; accepted 23 August 2016;

published online 13 September 2016)

The Thomson scattering diagnostic on MST records both equilibrium and fluctuating electron temperature with a range capability of 10 eV–5 keV. Standard operation with two modified commercial Nd:YAG lasers allows measurements at rates of 1 kHz–25 kHz. Several subsystems of the diagnostic are being improved. The power supplies for the avalanche photodiode detectors (APDs) that record the scattered light are being replaced to improve usability, reliability, and maintainability. Each of the 144 APDs will have an individual rack mounted switching supply, with bias voltage adjustable to match the APD. Long-wavelength filters (1140 nm center, 80 nm bandwidth) have been added to the polychromators to improve capability to resolve non-Maxwellian distributions and to enable directed electron flow measurements. A supercontinuum (SC) pulsed white light source has replaced the tungsten halogen lamp previously used for spectral calibration of the polychromators. The SC source combines substantial brightness produced in nanosecond pulses with a spectrum that covers the entire range of the polychromators. *Published by AIP Publishing.* [<http://dx.doi.org/10.1063/1.4962251>]

## I. INTRODUCTION

The MST Thomson scattering (TS) diagnostic uses scattered photon spectra to measure electron temperature fluctuations.<sup>1</sup> Traditionally data have been fit to Maxwellian distributions when determining the temperature. The recent diagnosis of energetic tails in the electron distribution function via MST's fast x-ray detector<sup>2</sup> has motivated adding the capability to appropriately fit non-Maxwellian and shifted distribution functions. The small étendue makes achieving these fits difficult and necessitates the optimization of the polychromator filter set.<sup>3,4</sup> Additionally, to quantify fluctuations and make an uncertainty determination, spectral calibrations that accurately characterize detector response must be regularly performed and checked.<sup>5</sup> A detector's gain is sensitive to temperature and bias voltage variations; consequently, the stability of these conditions is crucial.<sup>6,7</sup>

A hardware upgrade to the power supplies that bias the detectors of the system will be discussed in Section II. Section III will cover the enhancement of the system's capability to diagnose directed electron flows. Section IV will go over improvements to spectral calibrations. The paper ends with a summary of the results and the conclusions drawn from these results.

## II. HARDWARE UPGRADES TO DETECTION SYSTEM

The overall objective of this upgrade was to improve the maintainability, reliability, and usability of the detection

system. The panel that (i) acts as an interface between the avalanche photodiode detectors (APDs) and the digitizers and detector power supplies, (ii) contains circuitry for the power supply that biases the APDs, and (iii) sets the gains for the detectors will be removed in favor of a single cable feedthrough. Therefore, cables can pass unbroken to their destination, improving the fidelity of the signal traveling from the detectors to the digitizers. To compensate for the loss of function (ii) listed above, each APD will be powered from its own power supply. This increased modularity will improve the flexibility and robustness of the system. Function (iii) will be eliminated so that the gains can only be adjusted by altering an APD's pre-amplifier circuit.

An APD requires three operating voltages: +8 V, –8 V, and a high voltage (HV) bias in the range 270 V–420 V.<sup>6,7</sup> Each APD in the system will be powered from its own HV power supply. These HV power supplies will be housed in a rack and will be powered from a bus that distributes +8 V and –8 V to each HV power supply unit. Each unit then in turn outputs +8 V, –8 V, and HV bias to its respective APD.

The HV power supply circuit diagram was adapted from a diagram in Ref. 8. The HV power supply design employs a switching regulator with controlled transition times that efficiently reduce the high-frequency harmonic while boosting the input voltage (5 V after 8 V is fed into a 5 V regulator) to HV. A resonant Royer converter further reduces noise by minimizing the high-frequency harmonic in the power drive stage.<sup>8</sup> Fig. 1 graphically depicts the flow of the circuit of the HV power supply and the [supplementary material](#) includes its circuit diagram.

It was determined that the stability requirement for the HV bias was less than 123 mV variation. This value was obtained from the temperature stability requirement imposed during spectral calibrations and the APD's temperature coefficient

Note: Contributed paper, published as part of the Proceedings of the 21st Topical Conference on High-Temperature Plasma Diagnostics, Madison, Wisconsin, USA, June 2016.

<sup>a)</sup>skubala@wisc.edu

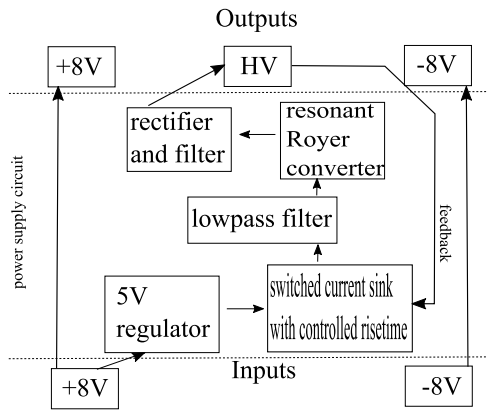


FIG. 1. Block diagram depiction of upgraded APD bias power supply circuit. One HV power supply module will power one APD.

for constant gain.<sup>5,6</sup> Fig. 2 shows results from long-time scale (duration of a typical run day) and short-time scale stability tests. These data indicate that the HV power supply meets the stipulated stability requirement.

Additionally, the noise output of a detector biased with an upgraded power supply was tested. The signal to noise ratio (SNR) for each APD is given by

$$SNR = \sqrt{\frac{N * QE}{F}}$$

where  $N$  is the number of photons detected,  $QE$  is the quantum efficiency, and  $F$  is the noise enhancement factor beyond

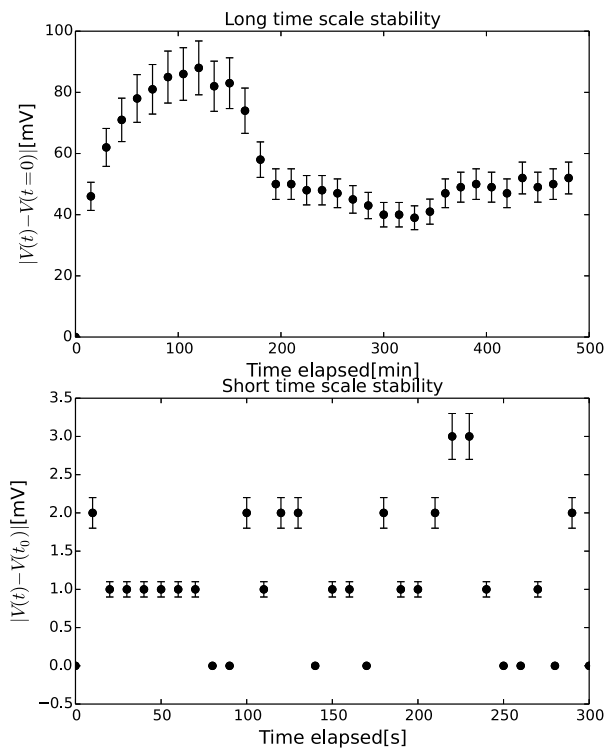


FIG. 2. The absolute value of the change in output voltage from the starting voltage is plotted over time. The long term stability data show that a warm up period is needed during which the voltage fluctuates by a relatively large amount for around two hours. The short time scale stability data were taken during the relatively stable region ( $t_0 = 315$  min). Both sets of data indicate that the stability requirement is satisfied.

Poisson statistics. The ratio  $F/QE$  is given by

$$\frac{F}{QE} = N_{APD} \frac{\sigma_{pulsed}^2 - \sigma_{dark}^2}{S_{APD}^2}$$

where  $\sigma_{pulsed}^2$  is the variance while the light source is pulsed,  $\sigma_{dark}^2$  is the variance when the light source is off, and  $S_{APD}$  is the signal of the APD.<sup>5</sup> Therefore, to determine if the use of upgraded HV power supplies resulted in a lower SNR, the dark variance of an APD was measured. The dark variance was the same for an APD biased with existing and new power supplies. In summary, the noise level and stability requirements on the upgraded power supplies are met.

### III. CAPABILITY TO RESOLVE DIRECTED ELECTRON FLOWS

Polychromators are employed by MST's TS system to partition scattered light by wavelength. Six of the polychromators use eight channels while the remaining use six channels. In both cases, the filter set typically used covers from approximately 715 nm–1065 nm. The scattered light signal collected by the detectors can then be fit to an expected spectral density profile, using  $\chi^2$  minimization to yield the best fit and the corresponding best estimate of the electron temperature.<sup>4</sup> While the system is set up so that it can effectively detect standard Maxwellian distribution functions, if the distribution function is shifted (as it would be for a directed electron flow) or non-Maxwellian, a longer-wavelength filter would provide the additional data necessary to fit such a distribution. The further the filter is placed from the laser line at 1064 nm, the better the capability to distinguish between non-Maxwellian and shifted Maxwellian distributions. Without this, fits to these two types of distributions could yield similar  $\chi^2$  values. Using simulations that accounted for the diminished response of the APDs at longer wavelengths, 1140/80 nm filters were selected and added to the filter set of eight polychromators, seven six-channel and one eight-channel.

Fig. 3 shows the instrument function (as defined in Ref. 5) of a six-channel polychromator where the long-wavelength

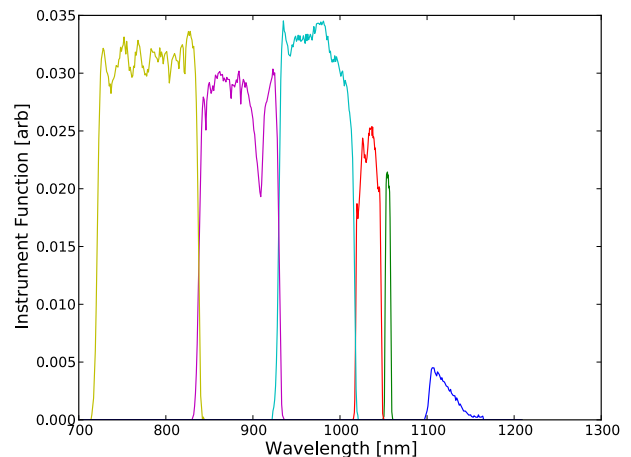


FIG. 3. Instrument function of a six-channel polychromator with a filter set that includes the long-wavelength, 1140/80 nm filter measured with super-continuum light source. The dip around 910 nm is due to impurities in the fiber that couples the light source to the polychromator.

filter has replaced the narrow filter centered around the laser line at 1064 nm. The relative drop-off of the instrument function response with increasing wavelength is a consequence of a silicon APD's diminished response at higher wavelengths,<sup>6,7</sup> but the ability to diagnose non-Maxwellian distributions is substantially enhanced.

#### IV. IMPROVED SPECTRAL CALIBRATION

In the past, a tungsten-halogen light source was used when performing spectral calibrations on the polychromators and APDs.<sup>5</sup> However, its SNR was insufficient. Next, an optical parametric oscillator (OPO) was used but had excessively large pulse-to-pulse variation.<sup>5</sup> The system now employs a supercontinuum white light source (SCLS), which combines substantial brightness produced in nanosecond pulses over the entire spectral range of the polychromators.<sup>9,10</sup>

The system is set up as shown in Fig. 4. Light is coupled to the monochromator via a fiber optic cable. The monochromator input slit couples directly into an integrating sphere. Two fibers are attached to the integrating sphere. One is coupled to the polychromator to be calibrated, the other to the absolutely calibrated reference detector (such as an APD). With this system, APD and absolutely calibrated detector signals are measured. Then combining these data with absolute calibration data, the instrument function, a product of the optical transmission of the polychromator and the  $QE$  of the APD, is generated.<sup>5</sup> A series of spectral calibrations performed with the SCLS indicate a statistical variation below 1%. Moreover, unlike the OPO, the SCLS allows for this calibration through the entire

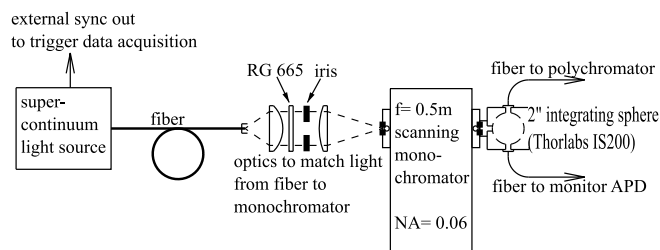


FIG. 4. Diagram of set up used for spectral calibrations with supercontinuum light source.

spectral range of a polychromator with a new long-wavelength filter.

#### V. SUMMARY

The upgraded power supplies described meet the stability and noise requirements and add modularity to the system. The addition of the long-wavelength filters to the polychromators improves the system's capability to detect directed electron flow and non-Maxwellian distributions. The supercontinuum light source's incorporation into the calibration procedure has enhanced the quality of the spectral calibrations via the brightness, reproducibility, and spectral range of its output.

#### SUPPLEMENTARY MATERIAL

See the [supplementary material](#) for the circuit diagram of the high voltage power supply and the digital format of the data shown in this paper.

#### ACKNOWLEDGMENTS

The authors thank Mikhail Reyfman, David Deicher, and Jacob Ziemke for their help. This work is supported by the U.S. Department of Energy Office of Science, Office of Fusion Energy Sciences program under Award Number DE-FC02-05ER54814.

- <sup>1</sup>J. Reusch, M. Borchardt, D. Den Hartog, A. Falkowski, D. Holly, R. O'Connell, and H. Stephens, *Rev. Sci. Instrum.* **79**, 10E733 (2008).
- <sup>2</sup>A. M. Dubois, J. D. Lee, and A. F. Almagri, *Rev. Sci. Instrum.* **86**, 073512 (2015).
- <sup>3</sup>T. N. Carlstrom, J. C. DeBoo, R. Evanko, C. M. Greenfield, C. L. Hsieh, R. T. Snider, and P. Trost, *Rev. Sci. Instrum.* **61**, 2858 (1990).
- <sup>4</sup>R. O'Connell, D. J. Den Hartog, M. T. Borchardt, D. J. Holly, J. A. Reusch, and H. D. Stephens, *Rev. Sci. Instrum.* **79**, 10E735 (2008).
- <sup>5</sup>H. D. Stephens, M. T. Borchardt, D. J. Den Hartog, A. F. Falkowski, D. J. Holly, R. O'Connell, and J. A. Reusch, *Rev. Sci. Instrum.* **79**, 10E734 (2008).
- <sup>6</sup>EG&G Canada Ltd., "Large Area Long Wavelength Enhanced Silicon Avalanche Photodiodes for General-Purpose Applications," C30956E data sheet, Jan 1. 1991.
- <sup>7</sup>C. L. Hsieh, J. Haskovec, T. N. Carlstrom, J. C. DeBoo, C. M. Greenfield, R. T. Snider, and P. Trost, *Rev. Sci. Instrum.* **61**, 2855 (1990).
- <sup>8</sup>J. Williams, "High voltage, Low noise, DC/DC converters," in *Application Note 118* (Linear Technology, 2008).
- <sup>9</sup>NKT Photonics, "SuperK COMPACT: Compact Single Mode White Light Source," SuperK\_COMPACT\_141217 data sheet, 2015.
- <sup>10</sup>R. Pasqualotto and A. Alfier, *Rev. Sci. Instrum.* **77**, 10E502 (2006).